Numerical simulation of cracking in structural masonry

J. G. ROTS
TNO Building and Construction Research
Delft University of Technology

Abstract

The paper presents the first results of a recently initiated research project on computational masonry mechanics. Examples are shown of (a) fundamental materials research that unravels the composite brick-joint action from basic properties, (b) fracture analyses on a semi-detailed level using assemblies of bricks and blocks bonded together by nonlinear interface elements at joint locations, and (c) global analysis of structural masonry whereby the effect of joints and cracks is smeared out in an anisotropic continuum model.

1 Introduction

The frequent use of the slogan "Brick is Beautiful" illustrates that masonry applications currently focus on decoration rather than structural aspects. In many buildings concrete frames and concrete walls provide the strength and stiffness, while the outer masonry is merely facade masonry without structural significance. Reasons for this are the lack of fundamental insight into the composite brick-joint behaviour and the consequent use of empirical models rather than rational models. This has led to a situation in which design rules and codes of practice for masonry are underdeveloped compared to those for popular structural materials like concrete and steel.
This situation was recognized by brick industries in the Netherlands and a research project "Structural Masonry" was initiated in 1989 in order to stimulate structural applications of masonry. The project covers the entire range from fundamental materials research to applied construction research via an integrated approach of experimental, analytical and computational methods. In this paper some of the first computational results will be shown. Emphasis will be placed on cracking, which is the major source of nonlinear behaviour in masonry.

2 Three approaches of different accuracy

Masonry is a composite material of bricks and joints. Depending on the degree of accuracy required versus simplicity desired, one can zoom in at various levels of abstraction and use models in which e.g.
- joints are represented by continuum elements;

- joints are represented by discontinuum elements;
- joints are smeared out.

In the first approach, Young's modulus, Poisson's ratio and, optionally, inelastic properties of both brick and joint material are taken into account. This enables the combined action of bricks and joints to be studied as though under a magnifying glass. In the second approach, again the bricks are modelled as continuum elements, but the joints are represented by line interface elements. With this approach, it is possible to consider the masonry as a set of elastic blocks bonded together by potential fracture lines at the joints. Accuracy is lost since Poisson's effect of the joints is not included. The third approach does not make a distinction between individual bricks and joints, but treats the masonry as an anisotropic composite such that joints and cracks are smeared out. This approach is attractive in global analysis of large-scale masonry structures.
A multi-purpose code like DIANA can be used for research on the above three levels. Examples will be shown in this paper.

3 Detailed study of brick-joint action

Masonry is composed of two materials having different properties. Usually, Young's modulus E_j of the joint material is significantly lower than Young's modulus E_b of the brick, while Poisson's ratio ν_j of the joint material is higher than Poisson's ratio ν_b of the brick. This departure in elastic properties of the constituents sets the overall behaviour of the composite. For instance, under uniaxial vertical compression the relatively soft mortar in between the bricks is pressed outwards, but is restrained by the relatively stiff brick, as shown in Fig. 1a. This implies that horizontal compressive stresses arise in the mortar and horizontal tensile stresses in the brick. The latter stresses govern ultimate failure under compression, i.e. the standard compressive test of Fig. 1 is in fact an indirect tension test. The masonry quality can be characterized by such tests in combination with simple formula based on linear-elasticity. In [2,7,13] such a formula was given for a fully 3D configuration. Here, a plane-strain configuration will be considered. The relation giving the ratio between horizontal tensile stress in the brick σ_{xx}^b and applied vertical compressive stress σ_{yy} under the assumption of linear-elastic behaviour and homogeneous deformations can then be derived to be:

$$\frac{\sigma_{xx}^b}{\sigma_{yy}} = -\frac{\nu_j(1+\nu_j)E_b - \nu_b(1+\nu_b)E_j}{(1-\nu_j^2)E_b t_b + (1-\nu_b^2)E_j t_j}\, t_j \tag{1}$$

in which t_b is the thickness (height) of the brick and t_j is the thickness (height) of the joint.
Some unresolved questions in this type of materials characterization are:

- The simple formula assume a homogeneous state of deformation and neglect the effect of stress concentrations at the edges.
- Nonlinear effects like delamination along the brick/joint interface and cracking and spalling of the brick may occur in the experiments but are disregarded in the formula.

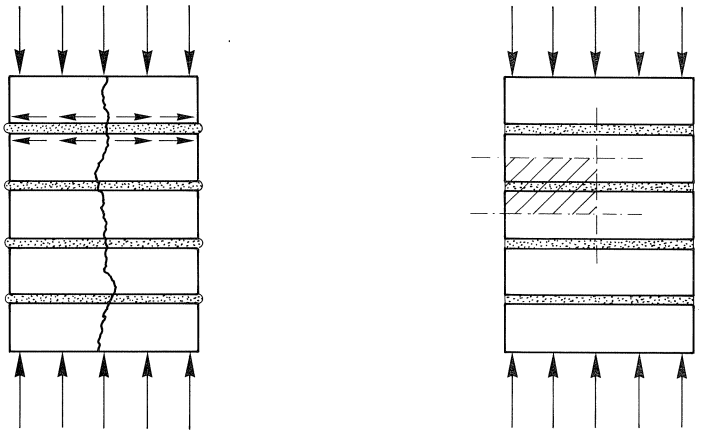

(a) (b)

Fig. 1. a. Masonry subjected to vertical compression.
Push-out of the relatively soft mortar is restrained by the brick. This leads to horizontal tensile stresses in the brick and results in an indirect tension failure.
b. Portion modelled in the plane-strain analysis (shaded).

- The mortar properties in the test are not well-defined due to complex drying conditions, leading also to imperfect contact along the brick/mortar interface. To circumvent this problem, Beranek and Hobbelman [2] proposed to perform additional tests using slices of neoprene as joint material, having well-defined properties and making smooth contact with the brick.

Figs. 2 and 3 show that finite element analysis can be used to support this materials research. The shaded part of Fig. 1b has been modelled using quadratic plane-strain elements. The brick dimensions were $50 \times 100 \times 200$ mm and the joint thickness t_j was 10 mm, i.e. 20% of the brick thickness $t_b = 50$ mm. The elastic properties of the brick were taken as $E_b = 18000$ N/mm^2, $\nu_b = 0.1$. Two linear-elastic analyses were undertaken, for mortar joint material with $E_j = 1300$ N/mm^2, $\nu_j = 0.2$ and for neoprene joint material with $E_j = 10$ N/mm^2, $\nu_j = 0.499$. In both analyses, an average vertical compressive stress $\sigma_{yy} = -1$ N/mm^2 has been applied while the vertical displacements at top and bottom were kept homogeneous by using dependence relations (tyings).

Fig. 2 gives an impression of the horizontal displacements and horizontal stresses for the analysis on the morter joint and Fig. 3 for the neoprene joint. Due to the extremely high Poisson's ratio and low Young's modulus of neoprene, the deformations are non-homogeneous over the entire specimen length and the neoprene is squeezed out like tooth paste. For the mortar joint, this effect is less pronounced. Here, the deformations in the interior of the specimen are almost homogeneous and a localized push-out effect occurs only near the edge.

The differences between mortar and neoprene are also reflected by the plots of the horizontal stresses σ_{xx}, which are almost equal to the principal stresses. For the mortar

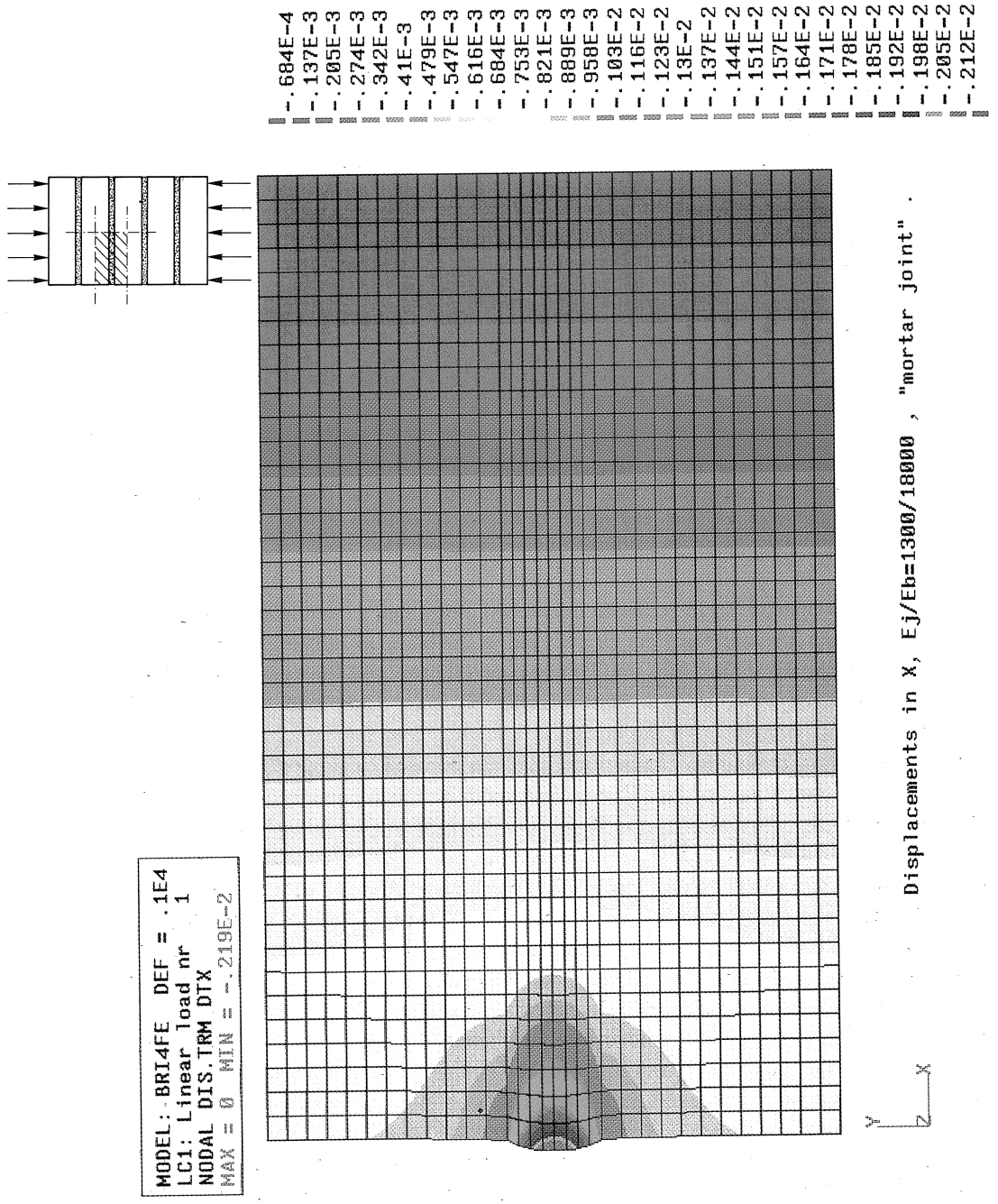

Fig. 2. Horizontal displacements for the analysis with mortar joint material. Analysis of the shaded part in Fig. 1b.

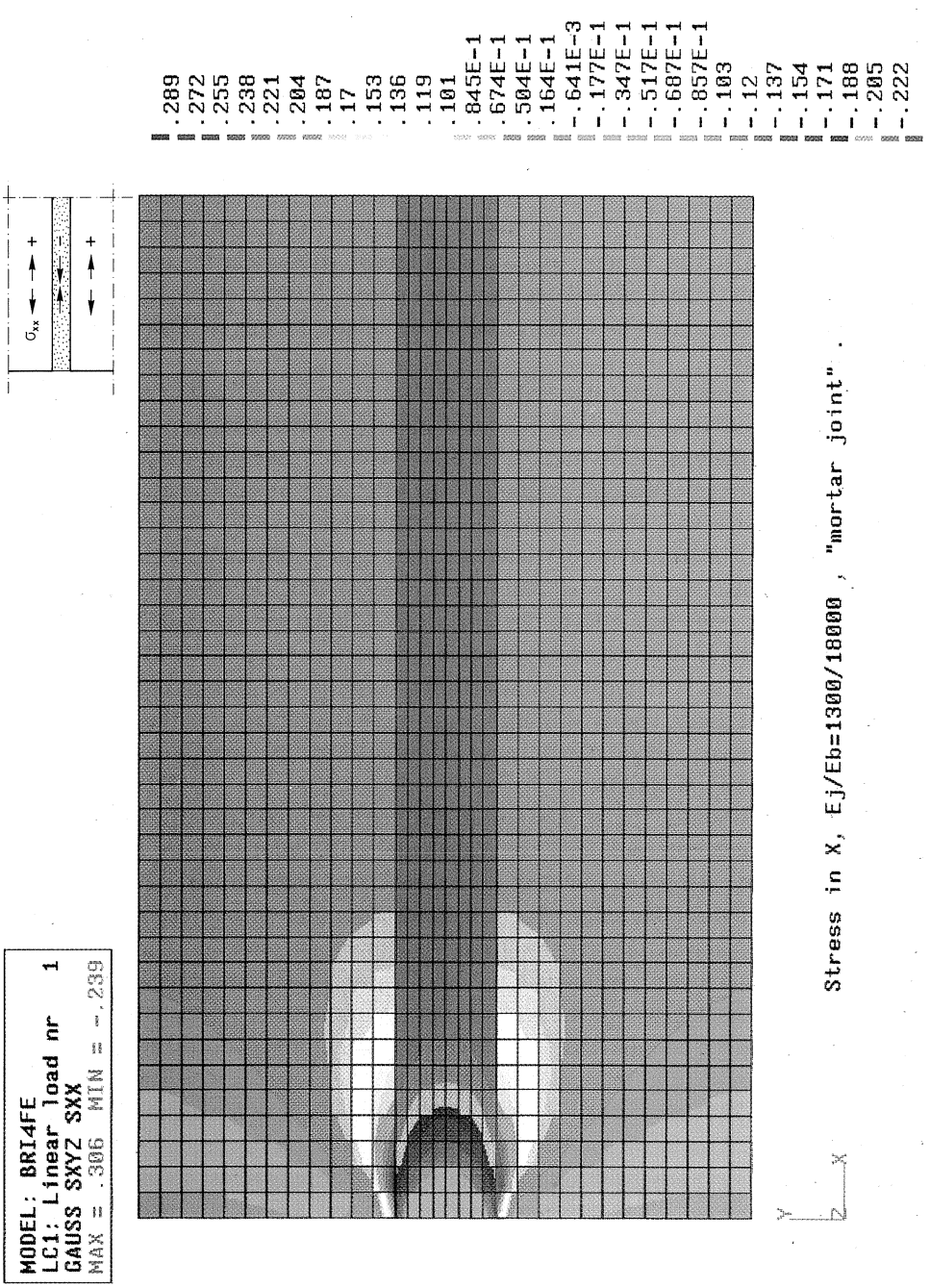

Fig. 2. – continued Horizontal stresses for the analysis with mortar joint material. Analysis of the shaded part in Fig. 1b.

joint an almost uniform tensile stress occurs over a large area in the interior of the specimen, whereas near the edge a complex stress concentration is visible along the brick/joint interface. The average horizontal tensile stress in the brick near mid-section is 0.0478 N/mm^2 and the peak tensile stress near the edge is 0.31 N/mm^2. The average value is very close to the value 0.0476 N/mm^2 obtained from eq. (1), indicating that the edge effect does not affect the behaviour in the interior of the specimen. For the neoprene joint not only an edge effect is observed, but also a disturbance of the stress field in the interior of the specimen. Now, the average horizontal tensile stress in the brick near mid-section is 0.28 N/mm^2, and the peak tensile stress near the edge is 0.49 N/mm^2. The average value now deviates from the value 0.2 N/mm^2 obtained from eq. (1), indicating that this equation which is based on homogeneous deformations is not correct in this case.

The preliminary conclusion is that edge effects and non-homogeneous deformations are important factors that cannot be ignored in masonry materials characterization. For the mortar joint, the peak stress in the brick amounts to 6.5 times the average stress and is likely to initiate cracking and spalling of the brick and/or delamination along the brick/joint interface, which has consequences for the objectiveness of the test as indicator of the material quality. The question is whether such damage propagates and dominates the outcome of the test, or whether it will be local only and arrested after a while. At the moment, nonlinear effects like smeared cracking and delamination [12] are introduced into the analyses to investigate this. The nonlinear analysis will furthermore reduce the sensitivity with respect to mesh refinement. In the present linear analyses, the peak stress becomes higher with increasing mesh refinement and the values mentioned herein merely serve the purpose of indicating the qualitative differences between mortar and neoprene.

For the neoprene joints, the peak stress in the brick amounts to only 1.8 times the average stress near mid-section. This explains why the pilot tests by Beranek and Hobbelman [2] on neoprene joints showed a nice and undisturbed indirect tension failure without undesirable edge effects. Indeed, their idea of indirect tensile measurements using neoprene seems to be attractive. However, a reservation must be made since the present analyses assume plane-strain. The analyses were repeated for plane-stress and the stress field for the mortar joint was about the same as for plane-strain, but the stress field for the neoprene joint turned out to be completely different as for plane-strain. The neoprene joint in plane-stress led to a much sharper stress concentration near the edge (0.72 N/mm^2 on an average of 0.1 N/mm^2), very similar as obtained for the mortar joint. This is of course due to the fact that the neoprene could now be squeezed out sideways in the out-of-plane direction. The actual test configuration lies somewhere in between plane-stress and plane-strain and is currently investigated in a fully three-dimensional analysis leading to the correct stress concentrations.

4 Semi-detailed analysis of masonry walls

For the majority of masonry structures, cracks will concentrate in the joints while the bricks remain intact. This lends support to a model that views the masonry as a set of linear-elastic blocks bonded together by nonlinear joints. In finite element analysis, this can be achieved by using linear-elastic continuum elements for the bricks and nonlinear discontinuum elements (interface elements) at the locations of the joints. The interface elements serve as potential discrete cracks. Initially, these elements get an equivalent normal and shear stiffness to model the joint in its elastic stage, but when the tensile strength is reached, a discrete crack opens up. The approach was used before in concrete mechanics [11] and has the advantage that it is also applicable to masonry without joint material, i.e. cohesionless stacks of bricks and blocks. Similarities exist with the distinct element method, which is being applied to masonry by Janssen [8]. Interface elements set a relation between tractions and relative displacements across the interface. With a line interface element for 2D analysis this relation is given by a two-by-two constitutive matrix that links the normal traction s_n and shear traction s_t to the relative normal displacement Δu_n and the relative shear displacement Δu_t across the interface:

$$\begin{bmatrix} \Delta s_n \\ \Delta s_t \end{bmatrix} = \begin{bmatrix} D_n & 0 \\ 0 & D_t \end{bmatrix} \begin{bmatrix} \Delta u_n \\ \Delta u_t \end{bmatrix} \tag{2}$$

Initially, the interface elements must represent the elastic normal and shear moduli of the joints, i.e. $D_n = E_j/t_j$ and $D_t = E_j/(2(1+\nu_j)t_j)$. When s_n exceeds the tensile strength f_{ct}, a crack is initiated and the stiffness moduli are changed according to a constitutive model for the crack. In this study, a tension-softening model was adopted for the behaviour normal to the discrete crack, while no shear stress transfer was assumed after cracking, i.e. $D_t = 0$ after cracking. The tension-softening model represents the effect that the tensile stress normal to the crack does not drop to zero immediately (elastic-brittle), neither does it remain at a constant level (elastic-plastic), but it decreases gradually with increasing crack opening displacement (elastic-softening). This model is controlled by three parameters, viz. the tensile strength f_{ct}, the shape of the softening diagram and the fracture energy G_f which is defined as the amount of energy required to create one unit of area of a crack and which is equal to the area under the softening diagram, see e.g. [10].

Figs. 4 and 5 show an example of a fracture simulation of a masonry wall. The wall is 1010 mm tall, 710 mm wide and 110 mm thick and was analysed before by Ali and Page [1]. The wall was subjected to a concentrated vertical load on a bearing platen of width 124.5 mm. The vertical displacements at the bottom side were assumed to be zero, but horizontal movement was allowed. Each half brick was modelled using four quadratic plane stress elements, not shown in Fig. 5 which displays only the contour lines. Quadratic interface elements with a lumped integration scheme [11] were placed not only at the positions of head joints and bed joints, but also in the middle of the bricks, between two head joints. In this way the majority of potential crack paths is captured,

Fig. 3. Horizontal displacements for the analysis with neoprene joint material. Analysis of the shaded part in Fig. 1b.

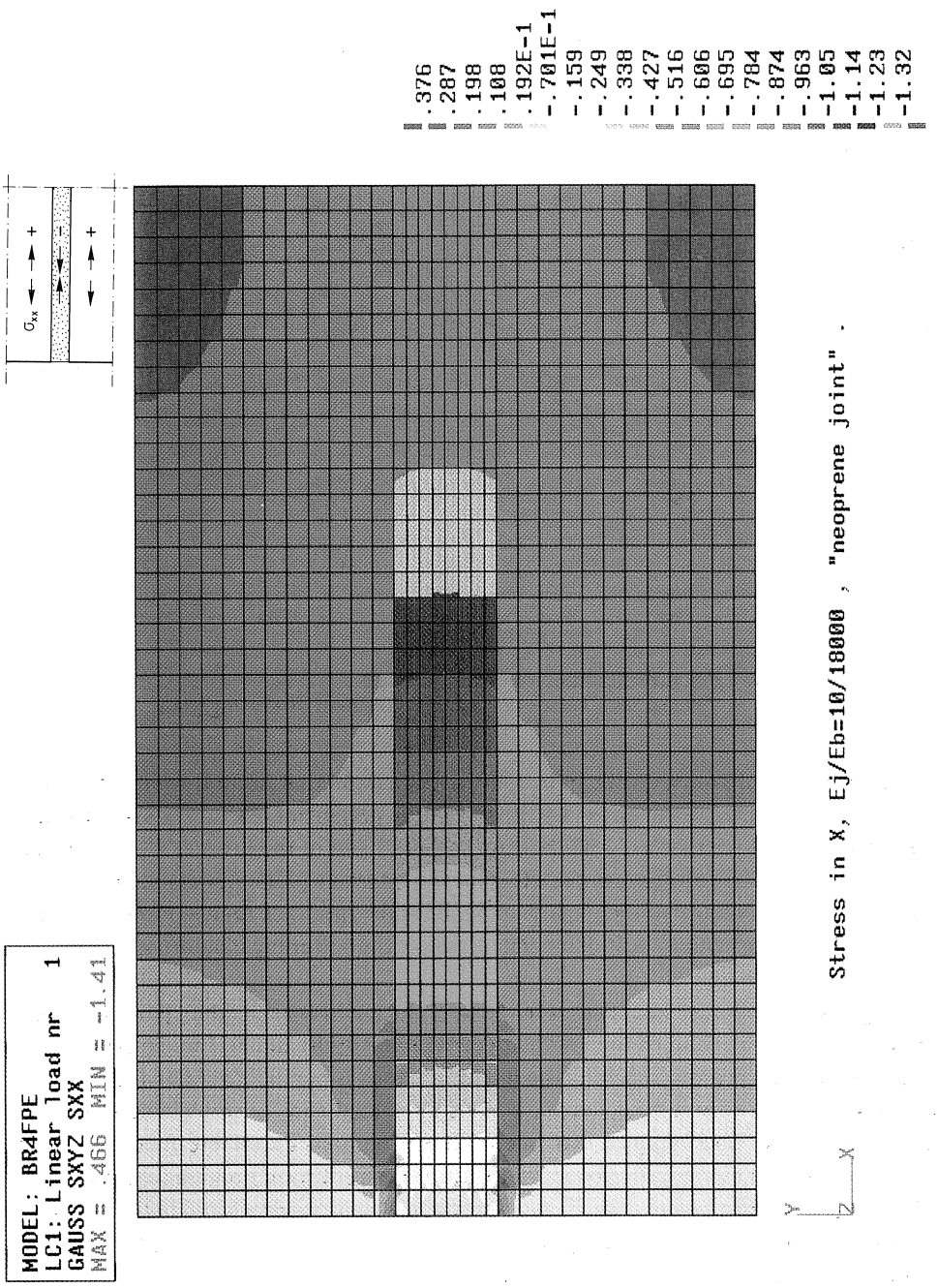

Fig. 3. – continued Horizontal stresses for the analysis with neoprene joint material. Analysis of the shaded part in Fig. 1b.

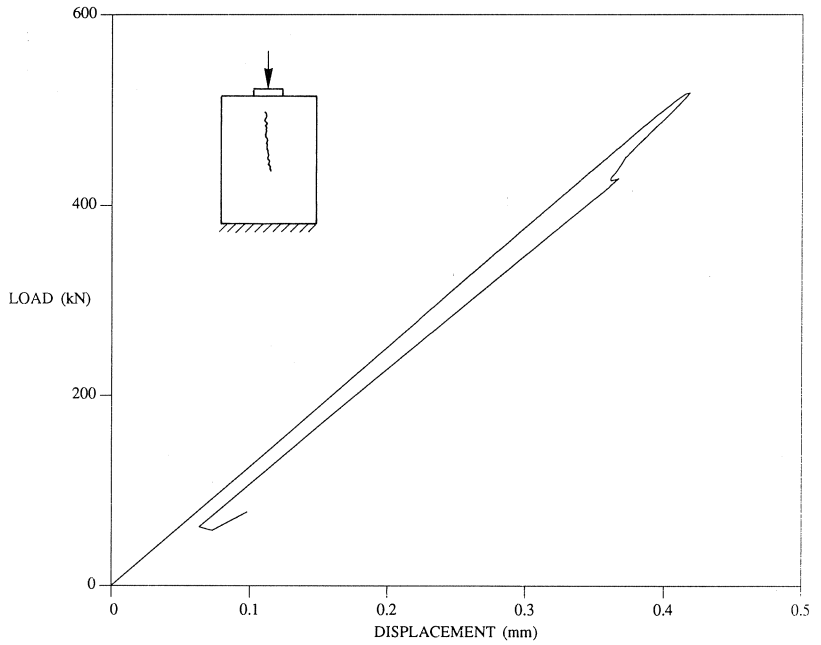

Fig. 4. Fracture simulation of masonry wall.
Vertical load versus vertical displacement at loading point.

viz. cracks in head joints, cracks in bed joints and cracks that jump from head joint to head joint right through the brick. The linear-elastic properties of the joints of thickness $t_j = 10$ mm were taken as $E_j = 7500$ N/mm^2, $\nu_j = 0.21$ and of the brick as $E_b = 15000$ N/mm^2, $\nu_b = 0.16$. The softening parameters for the interface elements in the bricks were taken as $f_{ct} = 1.2$ N/mm^2 and $G_f = 50$ J/m^2, and for the interface representing the joints as $f_{ct} = 0.78$ N/mm^2 and $G_f = 50$ J/m^2. The shape of the softening diagram was assumed to be linear.

Fig. 4 gives the computed behaviour in terms of the load versus loading point displacement. The rising portion of the curve appears to be almost linear, indicating that the effect of cracking prior to reaching the maximum load is negligible. After reaching the maximum load, a very sudden decrease of both the load and the displacement occurs. This "snap-back" phenomenon has been noticed before in concrete mechanics and requires a special arc-length procedure to control the solution process (De Borst [4]). The phenomenon indicates that the ratio between elastic energy stored in the structure at peak load versus fracture energy consumed in crack propagation is very high, resulting in a dangerous type of brittle fracture.

Fig. 5 gives an impression of the incremental displacements at various stages of the loading process. In the centre of the wall a splitting crack arises which propagates in a catastrophic manner after peak load. The computed crack path is straight and vertical,

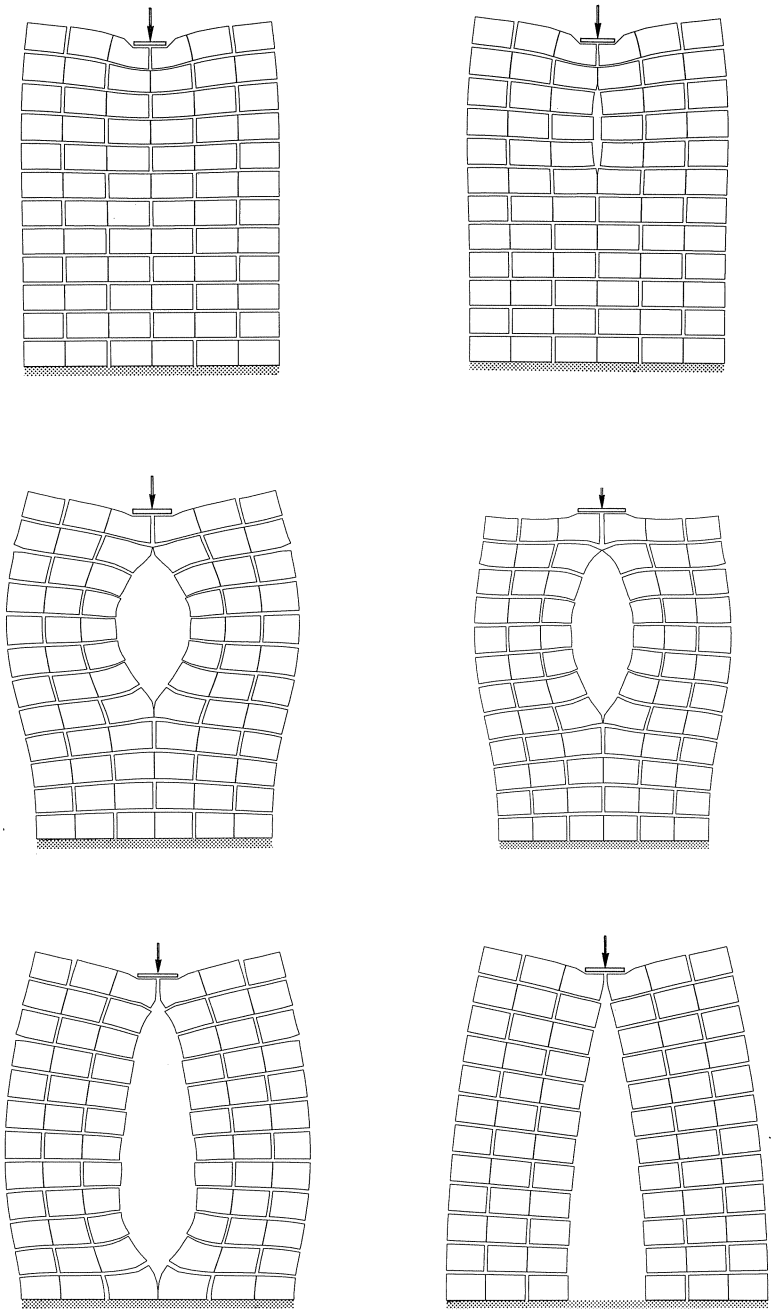

Fig. 5. Fracture simulation of masonry wall.
Incremental deformations in various load steps during the analysis, corresponding to Fig. 4. Bricks are represented as elastic blocks bonded together by nonlinear interface elements as potential discrete cracks.

indicating that the crack jumps from head joint to head joint right through the brick, rather than following a zig-zag path via head joint-bed joint-head joint etc. This behaviour is in line with the experimental findings [1].
Further information regarding these types of analyses, including variation studies of geometrical and material parameters are presented in [6] for vertical loading and in [5] for combinations of horizontal and vertical loading. Comparative studies with the distinct element method are described in [6,9].

5 Global model for masonry as a composite material

The previous approaches that distinguish between individual bricks and joints are not suited to global analysis of medium-and large-scale masonry structures. Fig. 6 shows an example of a wall with stress concentrations around openings, where it is not feasible to study the crack propagation along individual bricks and joints in a detailed manner. For such cases, there is a need for anisotropic continuum models in which the effect of joints and cracks is smeared out.
In this section it will be shown that the smeared crack concept proposed by De Borst and Nauta [3] and Rots et al. [10] for concrete can be easily extended to masonry. This

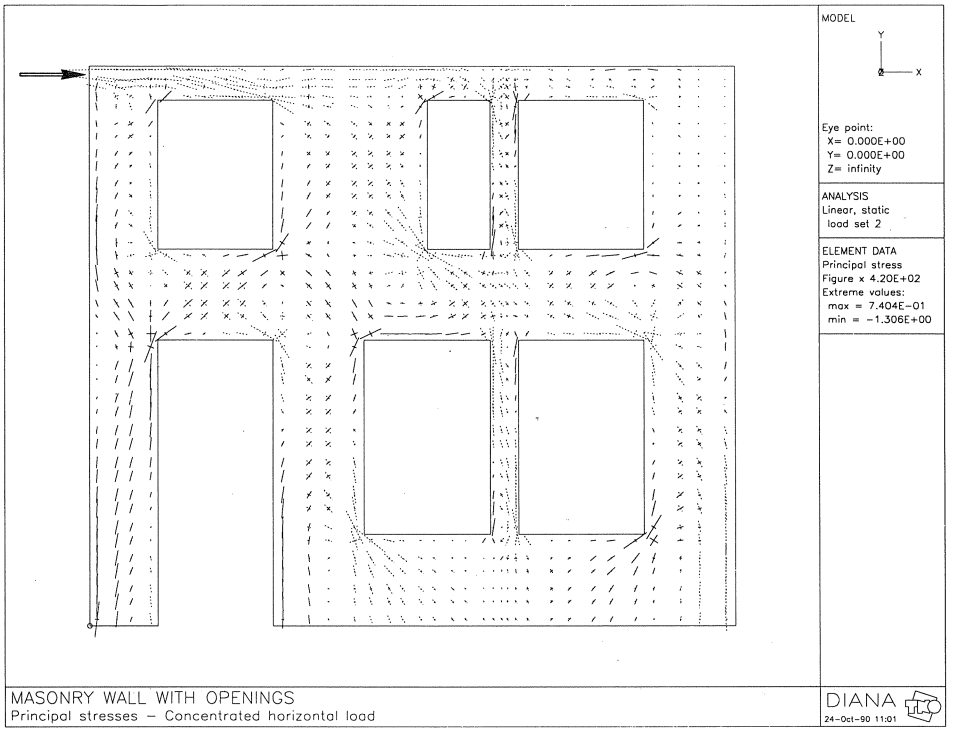

Fig. 6. Global analysis of structural masonry.
Principal stresses are shown (dotted compressive, dashed tensile). Stress peaks at corners will act as crack initiators.

concept starts from the assumption of a decomposition of the total strain increment $\Delta\boldsymbol{\varepsilon}$ into a part $\Delta\boldsymbol{\varepsilon}^{cr}$ of the crack and a part $\Delta\boldsymbol{\varepsilon}^{ma}$ of the solid material between the cracks:

$$\Delta\boldsymbol{\varepsilon} = \Delta\boldsymbol{\varepsilon}^{cr} + \Delta\boldsymbol{\varepsilon}^{ma} \tag{3}$$

The strain vectors in (3) relate to the global coordinate axes. In addition, a local crack strain vector $\boldsymbol{e}^{cr}$ and a local crack stress vector $\boldsymbol{s}^{cr}$ can be defined in the crack coordinate system. The relations between local and global vectors read

$$\Delta\boldsymbol{e}^{cr} = \boldsymbol{N}\Delta\boldsymbol{e}^{cr} \tag{4}$$

for the strains and

$$\Delta\boldsymbol{s}^{cr} = \boldsymbol{N}^{T}\Delta\boldsymbol{\sigma} \tag{5}$$

for the stresses. In (4) and (5) $\boldsymbol{N}$ is a transformation matrix that reflects the orientation of the crack. This matrix is assumed to be fixed upon crack initiation, so that the method belongs to the category of fixed smeared crack concepts.

The advantage of the strain-decomposition is that the constitutive relations of the solid material and the crack can be inserted separately, whereas most conventional methods directly start from an overall matrix. Denoting the constitutive matrices as $\boldsymbol{D}^{ma}$ and $\boldsymbol{D}^{cr}$, the stress-strain laws of the two components can be written as

$$\Delta\boldsymbol{\sigma} = \boldsymbol{D}^{ma}\,\Delta\boldsymbol{\varepsilon}^{ma} \tag{6}$$

and

$$\Delta\boldsymbol{s}^{cr} = \boldsymbol{D}^{cr}\,\Delta\boldsymbol{e}^{cr} \tag{7}$$

Using (3)–(7), the overall stress-strain law for the cracked material (either concrete, masonry or any other cohesive material) can be developed from the two components [3, 10]:

$$\Delta\boldsymbol{\sigma} = [\boldsymbol{D}^{ma} - \boldsymbol{D}^{ma}\boldsymbol{N}[\boldsymbol{D}^{cr} + \boldsymbol{N}^{T}\boldsymbol{D}^{ma}\boldsymbol{N}]^{-1}\boldsymbol{N}^{T}\boldsymbol{D}^{ma}]\,\Delta\boldsymbol{\varepsilon} \tag{8}$$

For concrete, $\boldsymbol{D}^{ma}$ is generally assumed to be the isotropic linear-elastic stress-strain matrix. The extension to masonry is made by using an orthotropic linear-elastic matrix instead. The orthotropy reflects the effect of bed joints and head joints. For concrete, the matrix $\boldsymbol{D}^{cr}$, which describes phenomena like tension-softening and crack shear in analogy to the discrete crack matrix (2) in the previous section, does not depend on the orientation of the crack. For masonry, this matrix becomes a function of the inclination angle α between the crack and the joints. Especially the tensile strength f_{ct} and the fracture energy G_f, which primarily define the tension softening term in $\boldsymbol{D}^{cr}$, are known to be different for cracks normal to bed joints and cracks perpendicular to bed joints, i.e. $f_{ct} = f_{ct}(\alpha)$ and $G_f = G_f(\alpha)$. In a separate paper, comparisons between this model and other smeared crack models for masonry (e.g. Ali and Page [1], Ma and Mai [9]) will be presented.

6 Concluding remarks

A brief overview of a research project on computational mechanics of structural masonry has been presented. Detailed studies of the brick-joint interaction show that edge effects and non-homogeneous deformations are important factors that cannot be ignored in masonry materials characterization via standard tests. A semi-detailed approach that represents the masonry as a set of elastic blocks bonded together by non-linear interface elements, has been demonstrated to be capable of simulating fracture propagation along bed joints, head joints and bricks. Finally, with a view to global analysis of structural masonry as an anisotropic composite, it has been shown that a smeared crack model based upon strain-decomposition can be easily extended to include the effects of initial orthotropy and crack-joint inclination angles.

Acknowledgements

The research is part of the project "Computational Masonry Mechanics" in CUR Committee A33 (CUR is the Centre for Civil Engineering Research, Codes and Specifications). Financial support from the Royal Dutch Association of Brick Manufacturers (KNB), the Netherlands Research Centre for Calcium Silicate Industry (RCK/CVK) and the Ministry of Economic Affairs (EZ) is gratefully acknowledged. The author is indebted to the graduate students A. C. Coenraads and S. M. Eijkman for their share in the analyses, which were performed using the DIANA finite element code with FEMVIEW postprocessing facilities.

References

1. Ali Sk. S. and Page A. W., Finite element model for masonry subjected to concentrated loads, ASCE Journal of Structural Engineering 114(8), 1761–1784, 1988.
2. Beranek W. J. and Hobbelman G. J., Mechanica-modellen voor steenachtige materialen, Part I "Model voor het materiaalgedrag", Part II "Model voor het constructiegedrag" (in Dutch), Research Reports, CUR Committee C77, Delft University of Technology, Department of Building Engineering, 1991.
3. De Borst R. and Nauta P., Non-orthogonal cracks in a smeared finite element model, Engineering Computations 2, 35–46, 1985.
4. De Borst R., Computation of post-bifurcation and post-failure behavior of strain-softening solids, Computers & Structures 25(2), 211–224, 1987.
5. Coenraads A. C., Numerieke detailberekeningen van penanten in metselwerk – Onderzoek naar modelleringsaspecten binnen DIANA (in Dutch), Graduate thesis, TNO-Bouw report BI-91-073/TU Delft report 25-2-91-2-07, 1991.
6. CUR Committee PA33, Preadvies numerieke metselwerkmechanica (in Dutch), Report 90-6, Centre for Civil Engineering Research, Codes and Specifications (CUR), Gouda, The Netherlands, 55 pp., 1990.
7. Francis A. J., Herman C. B. and Jerremy L. E., The effect of joint thickness and other factors on the compressive stress of brickwork, Proc. Second Int. Brick Masonry Conference, April 1970.
8. Janssen H. J. M., Progress reports "Computational Masonry Mechanics – UDEC", Eindhoven University of Technology, Department of Building Engineering, December 1990 and April 1991.

9. MA S. Y. A. and MAY I. M., A complete biaxial stress failure criterion for brick masonry, Proc. British Masonry Society, First Int. Masonry Conference, 115-117, 1986.
10. ROTS J. G., P. NAUTA, G. M. A. KUSTERS and J. BLAAUWENDRAAD, Smeared crack approach and fracture localization in concrete, HERON 30(1), 1-48, 1985.
11. ROTS J. G., Computational modeling of concrete fracture, Dissertation, Delft University of Technology, Department of Civil Engineering, 132 pp., 1988.
12. SCHELLEKENS J. C. J. and DE BORST R., Numerical simulation of linear and nonlinear fracture mechanics options to free edge delamination in laminated composites, HERON, this issue, 1991.
13. SCHULENBERG W., Theoretische Untersuchungen zum Bruchverhalten von gedrücktem Mauerwerk (in German), Mauerwerk-Kalender, 1984.